Metallophore profiling of nitrogen-fixing *Frankia* spp. to understand metal management in the rhizosphere of actinorhizal plants

Michael Deicke[a‡], Jan Frieder Mohr[a‡], Sébastien Roy[b], Peter Herzsprung[c], Jean-Philippe Bellenger[d], Thomas Wichard[a*]

[a] Friedrich Schiller University Jena, Institute for Inorganic and Analytical Chemistry, Lessingstr. 8, 07743 Jena, Germany

[b] Centre SÈVE, Département de Biologie, Faculté des Sciences, Université de Sherbrooke, QC, J1K 2R1, Canada

[c] UFZ - Helmholtz Centre for Environmental Research, department Lake Research, Brückstraße 3a, 39114 Magdeburg, Germany

[d] Centre SÈVE, Département de Chimie, Faculté des Sciences, Université de Sherbrooke, QC, J1K 2R1, Canada

‡These authors contributed equally to the manuscript

*corresponding author: Thomas.Wichard@uni-jena.de; Fax: +493641 948172; Tel: +493641 948184

Abstract

Frankia spp. are widespread nitrogen-fixing soil bacteria, which often live in symbiosis with a broad spectrum of hosts. Metal homeostasis plays a crucial role in the success of the symbiosis regarding the acquisition of essential trace metals and detoxification of potentially toxic elements. We have hypothesised that *Frankia* releases many organic ligands with a broad spectrum of affinity for essential and toxic metals. We coined the term 'ligandosphere' to describe the entirety of excreted metal complexing agents. Using metal isotope-coded profiling (MICP); metallophores of physiological important and toxic trace metals were identified by the addition of stable metal isotope pairs such as $^{54}Fe/^{58}Fe$, $^{63}Cu/^{65}Cu$, $^{64}Zn/^{66}Zn$ or $^{95}Mo/^{98}Mo$. Liquid chromatography coupled to a mass spectrometer revealed strong variations of the metallophore profile in between the 14 test-strains. In total, about 82 organic ligands were identified binding to one of the tested metals. The predicted sum formula of the major Fe binding ligands and MS/MS experiments suggested that several metallophore candidates have a similar molecular backbone. Growth experiments with a hyper-producer of metallophores revealed a positive relationship between metallophore production and the concentration of Cu in the growth medium. The present study provides the first comprehensive overview of the complexity of *Frankia*´s ligandosphere. It opens a path to deeper understanding of mechanisms that regulate metal homeostasis in frankiae. Deciphering these mechanisms is important since the fitness of actinorhizal plants and their potential in ecological restoration relies heavily on their symbiosis with frankiae.

43 **Significance to Metallomics**

44 Metal homeostasis plays a significant role in bacteria-plant interactions in the rhizosphere.

45 Bacteria can acquire trace metals through metallophores for metal-dependent processes like

46 nitrogen fixation and can contribute to alleviating metal stress. To understand how bacterial

47 metallophores contribute to metal management in a rhizosphere, it is necessary to determine the

48 entirety of metal complexing ligands. In this study, we have explored the metallophore

49 production by *Frankia* (Actinobacteria), a nitrogen-fixing soil bacterium, using metal isotope-

50 coded profiling. Our study has strong implications for the understanding of the role of bacteria

51 for the plant in trace metal acquisition and detoxification.

52

Introduction

Metal ions are essential for many enzymes, but an excess of metals can be toxic and reduce growth and development of a broad range of organisms. In bacteria, metal limitation activates pathways that are involved in the import and mobilisation of metals via metallophores, whereas an excess of metals induces efflux and storage[1]. Microorganisms in the rhizosphere, a micro-ecological zone in direct proximity of plant roots, provide many benefices to plants, such as defence against pathogens[2], increased macronutrient availability (e.g., N, P) as well as micronutrients (e.g., Fe, Cu, Zn, Mo) uptake[3]. For example, bacteria recruit directly iron for the metal-dependent enzymes, but they also assist in plant iron uptake[4]. Considering the bacteria mediated iron uptake in corn[4], the hypothesis iron-for-carbon[5] could be a widespread bacteria-plant interaction. Such interactions would likely strongly rely on bacterial metallophore production, which might influence trace metal bioavailability in the rhizosphere. Nitrogen-fixers like the ubiquitous soil bacteria, *Frankia* spp. (Actinobacteria), are of particular interest, as they form complex symbiotic interactions with a broad range of higher plants such as alder or sallow thorn, often along with ectomycorrhizal or arbuscular mycorrhizal fungi[6, 7]. After root infection, *Frankia* has access to a carbon source from the host and supplies nitrogen to the symbionts in return. Therefore, *Frankia* needs to acquire Mo and Fe for the nitrogenase reducing atmospheric N_2 to NH_3[8-10,11]. Nitrogen-fixing soil bacteria such as *Azotobacter vinelandii* utilise metallophores to increase the bioavailability of nitrogenase metal cofactors (i.e., Fe, Mo, V)[12], which are often bound by dissolved organic matter in the rhizosphere[13-15] and reduce the toxicity of unwanted metals (i.e., W)[16]. As many bacterial organic ligands, for example, the catecholate-type organic ligand protochelin can complex various metal cations (e.g., Fe^{3+}, Cu^{2+}, Zn^{2+}) or oxo-anions (e.g., molybdate, vanadate, tungstate), the use of metallophores for metal management could be a common strategy in bacteria[17]. Indeed, metallophores acquire many essential biometals by shaping the speciation of metals in the rhizosphere habitat to the benefice of their co-habiting bacteria and other organisms[18, 19]. Here, we use the term 'ligandosphere' to highlight the environment- and species-dependent bouquet of metallophores released by organisms of a specific habitat.

Although hundreds of siderophores were identified in the last decades[20], little is known about metallophore-based recruitment strategies for other metals. In *Frankia*, as in many other model bacteria, studies of metal-binding ligands were often limited to siderophore detection under Fe limited growth conditions using colourimetric approaches or investigations on heavy metal

4

85   tolerance, directly linked to their effect on bacterial physiology[21, 22]. More specific colourimetric

86   procedures have shown evidence for catecholate, and hydroxamate siderophores in various

87   *Frankia* isolates[23-25]. Boyer et al. (1999) found two potential siderophores, Frankobactin (782

88   *m/z*) and Frankobactin A (800 *m/z*)[26, 27] isolated from *Frankia* sp. strain 52065. NMR could

89   identify only substructures, the phenyl-oxazoline ring, some amino acids and the hydroxamate

90   units of the siderophores[28]. Genome mining of three isolates, ACN14a, CcI3 and EAN1pec,

91   revealed non-ribosomal peptide synthases (NRPS) that govern complex reactions in *Frankia*

92   including the assembly of phenols/catechol, oxazoline/thiazolines and hydroxamates[29]. The

93   NRPS domain suggested the sequence of 2,3-dihydroxybenzoate or salicylate followed by serine

94   or cysteine and a varying number of other amino acids, such as ornithine and threonine. Also, all

95   three *Frankia* genomes contain homologous NRPS-independent biosynthetic loci typical for an

96   aerobactin-like metallophore[29]. These results highlighted the potential diversity of metallophores

97   produced by *Frankia* spp.

98   We, therefore, raise the hypothesis that *Frankia* can release a strain-specific bouquet of organic

99   ligands, which facilitates the complexations of cations and oxo-anions for both recruitment and

100   detoxification of metals. Multiple metallophores might harbour similar structures, but their

101   affinities to, e.g. iron can vary. Such a 'ligandosphere' could evolve an advantage to recruit iron,

102   for example, in a changing environment from different resources. In this context, Hider and Kong

103   (2010) have already suggested distinguishing those ligands for solely iron complexation and

104   recruitment (primary siderophores) from those who are dedicated to non-classic function

105   (secondary siderophores) such as detoxification or just keeping metals in solution as a complex[20].

106   Metallophore-mediated tolerance mechanisms for potentially toxic heavy metals are essential for

107   bioremediation of contaminated sites[30-32]. The toxicity of metals mainly depends on their

108   concentration, speciation and bioavailability[33, 34]. Zinc and copper, for example, are necessary for

109   the function of various enzymes such as polymerase or cytochrome oxidase[35, 36], but also have a

110   strong toxic effect on microorganisms. Cu^{2+} ions can replace other metal ions in complexes and

111   can generate reactive oxygen species (ROS) by autoxidation or Fenton-like reactions that cause

112   oxidative stress and subsequent cell damage[37]. To avoid cell damage thought critical metal

113   concentrations, *Frankia* might feature different resistance mechanisms; immobilisation on the

114   cell surface, efficient metal-specific efflux systems and complexation by metallophores[22, 38]. In

115   this context, several *Frankia* strains are resistant against high Zn concentrations[39], but zinc

116 ligands (zincophores) and the Zn management are unknown in the genus *Frankia.* Anyway, it is

117 well known, that *Frankia* utilise all of the essential trace elements (Ni, Co, Cu, Se, Mo, B, Zn, Fe,

118 and Mn) and have a comparatively high percentage of metalloproteins, particularly in the more

119 metal resistant strains. *Frankia* has achieved similar levels of metal and metalloid resistance as

120 bacteria from highly metal-contaminated sites. More importantly, from a bioremediation

121 perspective, Furnholm and Tisa (2014) have outlined the importance to understand mechanisms

122 allowing the endosymbiont to survive and infect actinorhizal plants in metal contaminated soils[20].

123 For that reason the present study aims to determine the 'ligandosphere' in pure cultures of 14

124 *Frankia* strains for the complexation of selected metals such as Fe, Zn, Mo and Cu by using

125 metal isotope-coded profiling (MICP) supported by DeltaMS to identify the respective

126 isotopologues[40, 41] of unknown organic ligands in different growth media. *Frankia* serves thereby

127 as an ecologically important species for the rhizosphere microbiome and potential new model

128 system for interactions across the prokaryote-eukaryote boundary in soil similar to the well

129 investigated aquatic systems[42]. Overall, our elaborative screening sheds light on the dynamics of

130 the metallophore profile in the genus *Frankia* under standardised conditions and provides

131 information on how plants and associated fungi might involve microorganisms in their metal

132 homeostasis.

133

134 Experimental

135 Reagents and materials

136 All used ingredients of the bacterial growth media were purchased by Sigma Aldrich

137 (Taufkirchen, Germany) and VWR (Darmstadt, Germany). A Micro-Pure water purification

138 system (Thermo Scientific, Schwerte, Germany) provided the ultra-pure water (0.055 µS) for the

139 preparation of aqueous solutions. UHPLC-grade methanol, acetonitrile, water, ammonium acetate

140 and formic acid were purchased from VWR (Darmstadt, Germany). Cell tissue flasks and plastic

141 tubes were from Sarstedt (Nümbrecht, Germany).

142 Bacteria strains, culture media, growth conditions and protein quantification

143 All *Frankia* strains were provided by the Centre d'Étude de la Forêt culture collection (CEF),

144 Université Laval (Québec, Canada) except isolate DSM 44251 which was obtained from the

145 DSMZ (German Collection of Microorganisms and Cell Cultures, Göttingen, Germany). Two

146 growth media, BAP medium and the newly designed MI medium (metallophore inducing

147 medium), were used. The BAP medium was prepared as described in Bélanger et al. (2011)[43].

148 The MI medium was inspired by Murry et al. (1984)[44] and composed of (in g L^{-1}) KH$_2$PO$_4$,

149 0.953; K$_2$HPO$_4$, 0.592; NH$_4$Cl, 0.268; sodium propionate, 0.480; MgSO$_4$·7H$_2$O, 0.030;

150 CaCl$_2$·2H$_2$O, 0.010; trace metals (in g L^{-1}): H$_3$BO$_3$, 0.00286; MnCl$_2$·2H$_2$O, 0.00181;

151 ZnSO$_4$·7H$_2$O, 0.00022; CuSO$_4$·5H$_2$O, 0.00008; Biotin, 400 µg L^{-1}. Both media were

152 supplemented with FeCl$_3$ 5.0 × 10^{-7} mol L^{-1}, EDTA 5.0 × 10^{-6} mol L^{-1} and Na$_2$MoO$_4$·2H$_2$O 10^{-7}

153 mol L^{-1}. The final pH was adjusted to 6.8. Each culture was inoculated with a final protein

154 concentration of 10 µg mL^{-1} and cultivated in 650 mL uncoated polycarbonate cell culture flask

155 containing 200 mL culture medium. Flasks were incubated in static conditions at 30°C. After 25

156 days, 100 mL medium of each culture has been taken for analysis. The protein content of all

157 cultures was determined by homogenization, cell disruption and subsequent Roti®-Quant Protein

158 Assay (based on the Coomassie Bradford assay)[43].

Analytical process

159

160 Cultures were centrifuged at 3440 ×g for 10 min at 4°C. The supernatants (100 mL, 1.5 mL min^{-1}

161) were loaded on standard HLB-cartridges (200 mg sorbents, Oasis™ Waters, Milford, UK)

162 preconditioned with 6 mL MeOH and afterwards equilibrated with 8 mL water[16]. Upon loading,

163 the cartridges were eluted with 6 mL of 100% MeOH. An aliquot of each extract was used for the

164 universal Chrome Azurol S assay (CAS) to identify present Fe binding agents[45]. The remaining

165 extract was evaporated entirely under a nitrogen stream, and the sample residue was re-suspended

166 in 100 µL MeOH. For the subsequent Metallophore Isotope Coded Profiling (MICP) all extracts

167 were split into four equal aliquots. Each aliquot was spiked with 4 µL of a 10^{-2} mol L^{-1} stable

168 isotopes solution (ratio 1:1 of each pair: ^{54}Fe/^{58}Fe, ^{63}Cu/^{65}Cu, ^{64}Zn/^{66}Zn or ^{95}Mo/^{98}Mo) (Euriso-

169 top, Saint-Aubin Cedex, France) and measured by UHPLC-HRMS. The subsequent identification

170 of metal-binding complexes followed the workflow of MICP[40] coupled to a DeltaMS[41] automatic

171 peak detection tool. All listed total formulas were calculated using the inbuilt Thermo Xcalibur

172 Qual Browser software tool with a mass tolerance of less than 2 ppm considering the following

173 elements ^{1}H, ^{12}C, ^{16}O, ^{14}N, ^{32}S, ^{13}C, ^{23}Na, ^{54}Fe, ^{56}Fe, ^{58}Fe, ^{63}Cu, ^{65}Cu, ^{64}Zn, ^{66}Zn, ^{95}Mo, ^{98}Mo.

174 Confirmation and exclusion of formulas are exemplarily shown in Table S1 (using the example

175 $m/z = 782.3679$). Formulas with non-integer double binding equivalents (DBE) could be easily

176 excluded. Only components with $-10 \leq$ DBE - O $\leq +10$ were considered reliable[46]. Formulas can

177 be excluded if the O/N ratio was rather low, the number of DBE was low (cannot be a peptide),

178 or the number of S was high about N and O. Naturally formulas with minimum mass error were

179 most plausible. As a limitation, some formulas could not be completely excluded (for example

180 $C_{41}H_{56}O_{10}N_3S_1$). However, fragmentation experiments helped to confirm or to reject calculated

181 formulas.

UHPLC-ESI-HRMS measurements

183 Ultra-high-performance liquid chromatography (UHPLC) coupled with high-resolution mass

184 spectrometry (HRMS) was carried out using a Thermo (Bremen, Germany) UltiMate HPG-3400

185 RS binary pump, WPS-3000 autosampler which was set to 10°C and which was equipped with a

186 25 µL injection syringe and a 100 µL sample loop. The Kinetex® C-18 RP (50×2.1 mm; 1.7 µm)

187 column from Phenomenex (Aschaffenburg, Germany) was kept at 25°C using a TCC-3200

188 column compartment. Eluent A consisted of water, with 2% (v/v) acetonitrile and Eluent B was

189 90% acetonitrile (v/v). Both eluents were containing 1 mmol L^{-1} ammonium acetate[47]. The

190 chromatography was performed with a linear gradient (Table S2) and a constant flow rate of 0.4

191 mL min^{-1}.

192 Mass spectra were recorded with a Thermo QExactive plus Orbitrap mass spectrometer with

193 electrospray ionisation (ESI) source. Ionisation mode alternated between positive and negative

194 within 1 s and the mass window was set to 130-2000 *m/z*. The appending full scan settings were

195 as follows: resolution: 70,000; AGC target: 5.0×10^6; maximum IT: 200 ms. Following general

196 settings were used: sheath gas flow rate: 40; aux gas flow rate: 15; sweep gas flow rate: 0;

197 discharge current: 8.0 A; capillary temperature: 350°C; S-lens RF level: 33; vaporizer

198 temperature: 360°C; acquisition time frame: 0.2 - 9.5 min. All MS/MS measurements were

199 performed in a simultaneously mass detection arrangement with the following instrument

200 parameters: mass window 50-900 *m/z*, resolution: 280,000; AGC target: 3.0×10^6; maximum IT:

201 200 ms; collision energy: 25 eV. The general settings were adjusted like in full scan mode and the

202 scan period for each target mass was set two minutes around their belonging peak.

203

Copper tolerance and time-lapse experiments with *Frankia* sp. CH37

205 The Cu tolerance of *Frankia* strain CH37 was investigated in the presence of three different Cu

206 concentrations: 3.2×10^{-7}, 1.0×10^{-6} and 1.0×10^{-5} mol L^{-1} ($CuCl_2$). All treatments were inoculated

207 in cell flasks containing 200 mL MI medium with a final protein concentration of 10 µg mL^{-1}.

208   The cultures were monitored over a period of 53 days. Aliquots of 10 mL were taken at each

209   sampling point, centrifuged and the protein amounts were quantified. The remaining supernatant

210   (9.5 mL) was extracted with small HLB-cartridges (30 mg sorbents, Oasis™ Waters, Milford,

211   UK). All cartridges were preconditioned with 1 mL of MeOH and equilibrated with 1 mL water.

212   After loading the cartridge, the solid phase was washed with 1 mL of water. Compounds were

213   then eluted with 1 mL MeOH. Afterwards, the extracts were dried under a nitrogen stream,

214   resolved in 100 µL MeOH and measured with the UHPLC-HRMS-Orbitrap system.

215

Results and discussion

217   The metallophore profiles of 14 *Frankia* strains isolated from various host plants were very

218   variable (Table 1). Interestingly, culturing *Frankia* on propionate as a single carbon source (MI

219   medium) and a reduced vitamin-mix triggered the metallophore production compared to the

220   traditional applied growth medium (BAP medium). Elevated amounts of siderophores were

221   determined in the growth medium of the strain CH37, whereas the extracts of the known

222   siderophore producer strains, predicted based on genome analysis, ACN14a, Ea1-12, and CcI3[29]

223   reacted only moderately with the CAS assay. Surprisingly, the CAS assay indicated that only half

224   of the tested strains were able to release Fe binding organic ligands. As micronutrients such as

225   Fe, Zn and Mo are essential for the nitrogen fixer, we applied the metal isotope-coded profiling

226   (MCIP) to trace lower amounts of metallophores (Table 1) assuming false negative results by the

227   CAS assay due to a leak of sensitivity.

Metal isotope-coded profiling (MICP)

229   Metallophore candidates were determined upon addition of the isotope pairs ^{54}Fe/^{58}Fe, ^{63}Cu/^{65}Cu,

230   ^{64}Zn/^{66}Zn or ^{95}Mo/^{98}Mo (Fig. 1). In case of iron (^{54}Fe/^{58}Fe), regular features were considered as

231   potential metallophores, if two isotopologues of the mass spectrum showed the correct distance

232   of 3.9937 with an intensity ratio of 1:1 (deviation tolerance of 20%). Also, only those features

233   were selected with a signal to noise ratio of 10:1. The survey revealed that all strains were

234   releasing siderophores except two isolates (ACN10a and ACN12a). Non-detection of ligands in

235   both strains might also be related to low complex stability or short residence time during growth

236   or other recruitment strategies for Fe. These strains might also recruit iron by acquiring of not

237   own metallophores as recently demonstrated for the genus *Pseudomonas*[48]. Importantly, the

238   bouquet of the siderophores was strain specific and changed with the growth medium slightly, but

239   the ligands might be structurally related as many iron complexes eluted in a narrow window

240   between 2.2 - 3.0 min, which indicated a similar polarity of the separated molecules (Fig. 2A).

241   Overall, 35 potential siderophores were identified (Table S3), but 17 out of them have been

242   produced by a single strain initially isolated from *Hippophae rhamnoides* (sea buckthorn). Due to

243   its tolerance against strongly eroded, nutrient poor and sometimes salty soils, the plant is growing

244   on in coastal sand dunes[49] but also used for land reclamation.

245

246   Several criteria were defined for the reliable identification of new metallophores: first, Na- and

247   K-adducts of the metallophore, which shows the same isotopic signature as the initially identified

248   complex, point out the correct determination (Fig. 1B). Secondly, upon additional spiking of the

249   pair of isotopes, the ratio between the metal complex and the free ligands should have changed

250   significantly to the favour of the metal complex (Fig. S1). Finally, the HRMS measurements

251   reveal the sum formula with plausible DBEs (Table S1).

252   Following the defined criteria, the masses of the free ligand of the respective complex were

253   calculated and identified in the extracted ion chromatograms of an untreated sample. For

254   example, the signal of the ligands disappeared after adding the respected metal such as Fe and

255   conversely signals of the complexes increased (Fig. S1). In addition to the 35 Fe-complexes,

256   almost all strains released ligands complexing Cu (in total 28) with a molecular mass ranging

257   from 359 to 949 amu (Table S4). All determined Cu-ligands seem to bind cupric ions

258   preferentially compared to Fe. Moreover, a small number of stable zinc complexes were detected

259   in 5 out of 16 *Frankia* strains. However, the signal intensity was mostly weak except 694.1636

260   *m/z* and 841.3671 *m/z* for the ^{66}Zn isotopologues (Fig. 2B, Table S5). Surprisingly, no Mo-

261   complex were found under the chosen laboratory conditions indicating that *Frankia* recruits

262   added molybdate through a low-affinity transport system or it facilitates other sources of

263   molybdophores. The latter case is more likely as it was shown that Mo is mainly bound to

264   organic matter[14]. Interestingly, all detected metallophores seem to be metal-specific as just the

265   ligand **13** (796.3834 *m/z*) bound two metals (Fe and Cu) under the applied conditions.

266   **Determination of the sum formula**

267   The high-resolution mass spectra were used to estimate the sum formula. Hereby, the main

268   metallophores were selected by their signal intensity (intensity $\geq 1.24 \times 10^6$). The calculated mass

269 of the molecule ion deviated less than 2 ppm from the measured mass (Tables 2, 3). In a further

270 step, the given sum formulas were verified by calculating the number of carbon atoms from the

271 signal intensity of the ^{13}C peak and by the composition of the DBE (double bond equivalent)[46].

272 No sulphur was identified in the identified metallophores.

273 The proposed sum formulas of siderophore candidates **1-8** showed a very similar composition

274 (Table 2). All candidates have the same number of nitrogen atoms, and all other elements occur

275 in a very narrow range. Hereby, the molecular masses and sum formula of **2** and **3** fit very well

276 with the already published masses of Frankobactin and Frankobactin A, respectively. **2** and **3**

277 vary precisely in the mass of water as previously described by Boyer et al. [26]. Overall **1**

278 (817.2701 *m/z*), **2** (835.2785 *m/z*), and **3** (853.2891 *m/z*) differ just by 18.0105 amu in a

279 consecutive series (Table 2). The same loss of water was observed between **4** (831.2848 *m/z*) and

280 **5** (849.2961 *m/z*). Only **8** (915.3424 *m/z*) and **9** (958.3239 *m/z*) have a distinctively higher

281 molecular mass and accordingly more carbon, oxygen and nitrogen atoms (Table 2).

282 **1** and **4**, as well as **5** and **6**, differ just by a potential CH_2-group whereas **2** and **4** differ by a

283 potential CO group. In summary, we argue that those siderophores are derived from the same

284 biosynthetic pathway, and most likely, they are derivatives from Frankobactin. It seems

285 phonemically similar to the recently identified family of derivatives of protochelin - the key

286 metallophore in *A. vinelandii*[50]. Interestingly, the most abundantly formed Cu-complexes, **10 -**

287 **15**, have different masses over a broader range of polarity suggesting unique structural features

288 (Table 3, Fig. 2B).

289

Ligand classification

291 We have identified two different isotopic signatures of iron isotopologues (Fig. 3). The most

292 common iron isotopic signature has three significant isotopologues due to the complexation of

293 ^{54}Fe, ^{58}Fe (both after spiking) and ^{56}Fe, which was recruited from Fe-EDTA in the growth

294 medium. The differences were thus 1.9998 *m/z* between each isotopologue. The second observed

295 isotopic signature did not contain the isotopologue of ^{56}Fe. Therefore, we argue that *Frankia*

296 released at least two different types of organic ligands. Type I ligands possess a higher Fe affinity

297 or were produced in higher amounts than the type II siderophores. Therefore, type I ligands are

298 able to recruit ^{56}Fe form Fe-EDTA as expected from primary siderophores (Hider and Kong

299 2010). In addition, they have rapidly bound ^{54}Fe and ^{58}Fe upon their administration (Fig. 3A,

300 C)[20]. The isotopic signature of the molecule ion shows thus three isotopologues. However, no

301 ferric complexes of type II ligands were found in untreated extracts until [54]Fe and [58]Fe were

302 added (Fig. 3B,D). It is conceivable that type II ligands belong to the class of secondary

303 siderophores which might chelate other trace metals, or be used by the microorganisms for other

304 functions[20, 51, 52].

Determination of Frankobactin

306 Frankobactin is the only named siderophore released in *Frankia* so far[26]. The proposed sum

307 formulas of the siderophore candidates **1-8** show a very similar elementary composition.

308 Interestingly, the molecular masses of compound **2** and **3** (782 and 800 *m/z,* Tables 2, S1) fit very

309 well with the published masses of Frankobactin, and Frankobactin A produced by the *Frankia*

310 strains 52065 and CeSI5, respectively. Compounds, **2** and **3**, also differ by a loss of water as

311 previously observed for Frankobactin due to the ring opening of oxazoline[26]. In our study, a

312 Frankobactin-like siderophore was found in strain CH37 which is phylogenetically related to the

313 isolate CeSI5[53]. The data also support the previous genome mining-based approach[29], which

314 suggested three NRPS-based biosyntheses of siderophores ranging from 610 to 900 amu

315 including unknown substructures. Our study paves the way for selecting the ideal strain for

316 purification of Frankobactin and related ligands for structure elucidation and eco-physiological

317 testing.

318

MS/MS experiments for further structure elucidation

320 To gain insights into the molecular structure of the metallophores, MS/MS experiments of the

321 main candidates of Fe and Cu metallophores were performed. The spectra of **1-5** show a similar

322 fragmentation pattern, which is different to those of **6-9**. Starting from the C-terminal end, the

323 MS/MS data for **1-5** revealed a neutral loss of formyl-hydroxyl-ornithine (176.0785 *m/z*)

324 followed by a neutral loss of ornithine (114.0793 *m/z*) and a acetyl-hydroxyl-ornithine (172.0846

325 *m/z*), as also found in many other metallophores (Table 4, Fig. 4A)[20, 29, 54]. The resulting

326 fragments for **1** were 177.0867 *m/z*, 291.1657 *m/z* and 435.2561 *m/z* (including a potential loss of

327 CO). Also, a neutral loss of threonine (101.0475) directly linked to the acetyl-hydroxyl-ornithine

328 was identified (Fig. 4A). In **6,** the formyl-acetyl-ornithine seems to be replaced for hydroxyl-

329 acetyl-ornithine (190.0950 *m/z*).

330 The phenyl-oxazoline ring and its opening were confirmed by the characteristic salicylate

331 fragments and identified for **1-5** (Fig. 4B)[55-57]. It is noteworthy that fragments of the phenyl-

332   oxazoline group were not occurring if default settings for MS/MS experiments were used. The

333   direct molecular link between the amino acid chain and the phenyl-oxazoline ring are still unclear

334   and might be the reason for the differences observed between **1, 2** and **4**, aside from the mass

335   difference of water in **3** and **5**. In general, the MS/MS spectra have often shown neutral losses of

336   water, CO and NH_3, which are characteristic for peptide fragmentation. Overall, the

337   fragmentation pattern supports the assumption that **1-5** share the same molecular backbone

338   (Table 4).

339

Cu- and Fe-complexes formed during bacterial growth in the presence of high levels of Cu

341   MICP allowed us identifying complexes for a targeted analysis during a time-lapse experiment of

342   bacterial growth estimated by protein content. *Frankia* sp. strain CH37 was thus selected for its

343   relatively high metallophore production of ^{56}Fe-siderophores. At 1.0×10^{-6} mol L^{-1} Cu, the

344   growth curve phenocopied growth under the standard Cu concentration (3.2×10^{-7} mol L^{-1}). After

345   a short lag phase, the bacterial population grew exponentially with an abruptly ceases around day

346   15, followed by a typical decline phase. Some studies observed a more extended lag period, but

347   the growth curve, in general, was similar to previously reported ones[26] (Fig. 5A). In the presence

348   of elevated amounts of Cu (1.0×10^{-5} mol L^{-1}), bacteria did not grow in all biological replicates

349   suggesting that the detoxification not work under this conditions. However, moderately high Cu

350   concentrations of 1×10^{-6} mol L^{-1} allowed bacterial growth. The amount of siderophore **4**

351   increased along the exponential bacterial growth until day 15 (Fig. 5B). The siderophore seemed

352   to be taken up or catabolised by the bacteria since its concentration decreased from day 15 and

353   was no longer produced (or at a lower rate than the uptake) during the decline phase. A similar

354   metallophore profile was observed in time-lapse experiments with *A. vinelandii* under nitrogen-

355   depleted conditions. Here, few cells produced a significant amount of protochelin during the lag

356   phase to increase the iron-bioavailability before exponential growth[47].

357   In contrast to the ferric complex, the measured amount of the Cu-complex **13** did not follow the

358   time lapse of bacterial growth. For both tested Cu concentrations in the medium, the level of the

359   Cu-complex increased steadily until day 32 to an equilibrium concentration (Fig. 5C). Also, the

360   overall amount of Cu-complexes accelerated with the higher concentration of Cu in the growth

361   medium as also observed for Fe. The results correspond very well with earlier studies on *A.*

362   *vinelandii,* which releases a higher amount of organic ligands in the presence of elevated

363   concentrations of toxic metals like tungstate[16]. Due to this fact, the increase of copper binding

13

364 ligands in *Frankia* might be the reason why growth is not influenced in the presence of elevated

365 amounts of Cu. In this context, studies have recently identified several siderophore-producing

366 microbial taxa in response to heavy metal contamination[58].

367 We thus suggest that Cu-complexation can contribute to the heavy metal resistance in *Frankia*

368 besides other detoxification mechanisms. The number of metals present might regulate

369 metallophore production as part of the homoeostasis, and directly influence the metallophore

370 bouquet in the ligandosphere of these bacteria. Indeed, biosynthesis pathways of metallophores

371 are often induced in the presence of potentially toxic metals such as in *Pseudomonas*[59]. Large

372 amounts of metallophores provide bacteria with extracellular protection by complexing metals[34,

373 60] which ultimately reduces metal uptake by preventing metal diffusion into bacteria via porins[61].

374 Future short-term uptake experiments have to verify if the identified metallophores can control

375 the uptake of Fe, Cu and other metals such as Zn.

376

Conclusion

378 *Frankia* requires a constant supply of essential metals like iron to assemble the iron- and

379 molybdenum-dependent nitrogenase. The survey of a biodiverse panel of *Frankia* strains showed

380 plastic, strain-specific, and dynamic metallophore profiles determined by MICP and DeltaMS.

381 Overall, Frankiae is capable of producing a wide variety of chelators that could potentially

382 contribute to the natural ligand pool in the rhizosphere. Depending on the strain and growth

383 media, as many as to 17 metallophores were detected in the culture supernatant. While strain

384 CH37 was found to be a metallophore hyper-producer, other strains released only a few

385 metallophores or even no metallophore to the growth medium. The profiles we observed also

386 differed sharply in their composition depending on the growth medium (carbon source),

387 indicating that very dynamic changes occur in the *Frankia* ´ligandosphere´. Frankiae seems to

388 provide specific pools of metallophores that preferentially complex Fe, Zn, or Cu. Surprisingly,

389 no Mo-binding ligand was identified, although, like Fe, it is an essential element for the Mo-

390 dependent nitrogenase.

391 It is thus tempting to hypothesise that the mutualistic interactions between frankiae,

392 ectomycorrhizal fungi and alder within its rhizosphere are based on both a nitrogen-for-

393 molybdenum and iron-for-carbon dependencies under diazotrophic conditions. Frankiae will

14

394 deliver ammonium and recruits iron if the other organisms recruit Mo and deliver carbon. In any

395 case, further experiments would need to be conducted under strict diazotrophic conditions and

396 more challenging molybdenum sources (Mo complexed to organic matter and Mo-oxides

397 complexes) to elucidate whether or not, and under which circumstances, frankiae or associated

398 fungi produce molybdophores

399 Recorded MS/MS data suggest the existence of a similar molecular scaffolding of the main

400 siderophore candidates, one that contains substructures such as ornithine and the already-known

401 open and closed forms of the phenyl-oxazoline ring. Our study also revealed that the production

402 of ligands for Fe and potentially toxic metals such as Cu are regulated quite differently. Based on

403 these results, we suggest a ligand-mediated Cu resistance mechanism (as previously shown for

404 other organism and metals) coexists with other resistance mechanisms such as efflux systems and

405 detoxification processes that occur at the cell surface.

406 Our results highlight that *Frankia* possesses a variety of metallophores that are produced

407 dynamically, and adaptively to manage metal stress, ultimately leading to the acquisition, and/or

408 detoxification. In the rhizosphere, where *Frankia* and its host plants are exposed to multiple

409 metal stresses, metallophore-based management of metals would likely contribute to the fitness

410 of both symbionts, as well as provide essential elements to maintain the performance of their

411 nitrogen-fixing symbiosis. Our survey paves the way for targeted investigations into

412 metallophore-mediated elemental acquisition and detoxification in *Frankia* and its host plants in

413 both natural, and anthropised environments.

Conflicts of interest

There is nothing to declare.

Acknowledgements

426 **Tables**

427 **Table 1**: CAS assay and MICP based determination of metallophore production in 14 *Frankia*

428 strains during stationary growth. The preliminary screening revealed the effect of the tested

429 growth media (using BAP or MIM) on the siderophore production. Using the CAS assay, the

430 relative amount of siderophores is indicated by (+++) strong, (++) moderate and (+) weak and

431 compared with Fe-isotope coded profiling (Fe-icp) as well as Cu-icp and Zn-icp. No

432 molybdophore was identified.

433

Strain	Host	CAS assay (BAP)	CAS assay (MIM)	Fe-icp (MIM)	Cu-icp (MIM)	Zn-icp (MIM)
ACN10a	*Alnus crispa*				1	
ACN12a	*Alnus crispa*				1	2
ACN14a	*Alnus crispa*		+	5	6	1
CcI3 (Univ. Laval)	*Casuarina cunninghamiana*			1	4	
CcI3 (Lab. Boyer)	*Casuarina cunninghamiana*	+	+	5	3	1
CH37	*Hippophae rhamnoides*	+	+++	19	28	1
CPI1	*Comptonia peregrina*				1	
Cg70.4	*Casuarina glauca*			1	2	
Cg70.9	*Casuarina glauca*			1	1	
Cj1-82	*Casuarina junghuniana*			4	1	
Ea1-12	*Elaeagnus angustifolia*	+	++	5	1	
DC12	*Datisca cannabina*			2		
BCU 110501	*Discaria trinevis*		+++	8	1	1
DSMZ 44251	*Alnus rubra*			3	1	

434

435

17

436   **Table 2**: Calculated total formulas of the ^{56}Fe-complexes and their ligands extracted from the

437   supernatant of *Frankia* strain CH37. High-resolution masses were determined after adding ^{56}Fe to

438   the solid phase extracts.

Compound number	^{56}Fe^{III}-Complex [m/z]*	Ligand [m/z]	Proposed total formula [M-2H +^{56}Fe^{III}]$^+$	Proposed total formula [M+H]$^+$
1	817.2701	764.3572	$[C_{33}H_{47}O_{12}N_9{}^{56}Fe^{III}]^+$	$[C_{33}H_{50}O_{12}N_9]^+$
2	835.2785	782.3679	$[C_{33}H_{49}O_{13}N_9{}^{56}Fe^{III}]^+$	$[C_{33}H_{52}O_{13}N_9]^+$
3	853.2891	800.3783	$[C_{33}H_{51}O_{14}N_9{}^{56}Fe^{III}]^+$	$[C_{33}H_{54}O_{13}N_9]^+$
4	831.2848	778.3729	$[C_{34}H_{49}O_{12}N_9{}^{56}Fe^{III}]^+$	$[C_{34}H_{52}O_{12}N_9]^+$
5	849.2961	796.3835	$[C_{34}H_{51}O_{13}N_9{}^{56}Fe^{III}]^+$	$[C_{34}H_{54}O_{13}N_9]^+$
6	863.3119	810.3997	$[C_{35}H_{53}O_{13}N_9{}^{56}Fe^{III}]^+$	$[C_{35}H_{56}O_{13}N_9]^+$
7	803.2897	750.3784	$[C_{33}H_{49}O_{11}N_9{}^{56}Fe^{III}]^+$	$[C_{33}H_{52}O_{11}N_9]^+$
8	915.3424	862.4301	$[C_{39}H_{57}O_{13}N_9{}^{56}Fe^{III}]^+$	$[C_{39}H_{60}O_{13}N_9]^+$
9	958.3239	905.4109	$[C_{38}H_{54}O_{14}N_{12}{}^{56}Fe^{III}]^+$	$[C_{38}H_{57}O_{14}N_{12}]^+$

439

440

441 **Table 3**: Calculated total formulas of the ^{63}Cu complexes and their ligands extracted from the

442 supernatant of *Frankia* strain CH37.

Compound number	^{63}Cu^{II}-Complex [m/z]	Ligand [m/z]	Proposed total formula [M-H+^{63}Cu^{II}]$^{+}$	Proposed total formula [M+H]$^{+}$
10	619.1816	558.2680	$[C_{26}H_{34}O_7N_7{}^{63}Cu^{II}]^{+}$	Not found
11	681.2169	620.3033	$[C_{28}H_{40}O_9N_7{}^{63}Cu^{II}]^{+}$	$[C_{28}H_{42}O_9N_7]^{+}$
12	605.1619	544.2483	$[C_{24}H_{36}O_{11}N_3{}^{63}Cu^{II}]^{+}$	$[C_{24}H_{38}O_{11}N_3]^{+}$
13	857.2962	796.3834*	$[C_{34}H_{52}O_{13}N_9{}^{63}Cu^{II}]^{+}$	$[C_{34}H_{54}O_{13}N_9]^{+}$
14	551.1046	489.1832	$[C_{19}H_{28}O_{11}N_4{}^{63}Cu^{II}]^{+}$	$[C_{19}H_{29}O_{11}N_4]^{+}$
15	560.1687	499.2552	$[C_{26}H_{33}O_6N_4{}^{63}Cu^{II}]^{+}$	$[C_{26}H_{35}O_6N_4]^{+}$

443 Note: *This ligand formed stable complexes with both Fe and Cu in the growth medium under

444 the selected conditions.

445

19

446   **Table 4:** Fragmentation series for five siderophore candidates

Fragmentation series	Siderophore candidates				
	1	**2**	**3**	**4**	**5**
Molecular ion	**764.3566**	**782.3664**	**800.3543**	**778.3712**	**796.3808**
1	588.2780	606.2879	624.2745	602.2935	620.3019
2	474.1986	492.2086	510.1960	488.2144	506.2231
3	302.1137	320.1237	338.1147	316.1288	334.1388
4		219.0765			

447

448

449 **Legends**

450 Fig. 1: (**A**) Workflow and analytical process of the screening for metallophores in the genus

451 *Frankia*. (**B**) Representatives mass spectrum of a siderophore obtained by ESI-Orbitrap-HRMS.

452 Besides the molecular ions (*m/z* 861 and *m/z* 865), the doubly charged and sodium adduct of the

453 Fe-complex are shown.

454 Fig. 2: Plot of *m/z* values of all detected metallophores over retention time. (**A**) Fe-complexes

455 determined in *Frankia* spp. grown in BAP or MI medium. (**B**) Cu- and Zn complexes determined

456 in *Frankia* spp. grown in MI medium.

457 Fig. 3: Characteristic isotopic signature of the ferric complexes for organic ligands of (**A, C**) type

458 I and (**B,D**) type II. (**A**) Type I ligands recruit iron from Fe-EDTA. (**B**) Type II ligands do not

459 complex iron under standard growth conditions in the presence of Fe-EDTA. Upon addition of

460 ^{54}Fe and ^{58}Fe to the extracts, both (**C**) type I and (**D**) type II ligands form iron complexes showing

461 the isotopologues in the ratio 1:1.

462 Fig. 4: The electrospray MS/MS mass spectrum (positive mode) for ligand **2** (782 *m/z*). (**A**) A

463 typical fragmentation series of the backbone is shown at the collision energy 25 eV. (**B**) The

464 experiment at the collision energy 20 eV of *m/z* 782 reveals the characteristic fragmentation of

465 the phenyl-oxazoline-ring.

466 Fig. 5: Time lapse of the growth of *Frankia* sp. strain CH37 in MI medium. (**A**) Growth curves

467 are based on total protein content and observed under standard conditions at low, high and toxic

468 Cu concentrations. (**B**) The relative amounts of the Fe-complex **4** (831 *m/z*) and (**C**) Cu-complex

469 **13** (681 *m/z*) are shown.

470

471

472

References

1. P. Chandrangsu, C. Rensing and J. D. Helmann, Metal homeostasis and resistance in bacteria, *Nat. Rev. Microbiol.*, 2017, **15**, 338.
2. E. T. Kiers and R. F. Denison, Sanctions, cooperation, and the stability of plant-rhizosphere mutualisms, *Annu. Rev. Ecol., Evol. Syst.*, 2008, **39**, 215-236.
3. P. S. Kidd, V. Álvarez-López, C. Becerra-Castro, M. Cabello-Conejo and Á. Prieto-Fernández, in *Adv. Bot. Res.*, eds. A. Cuypers and J. Vangronsveld, Academic Press, 2017, vol. 83, pp. 87-126.
4. R. Hermenau, K. Ishida, S. Gama, B. Hoffmann, M. Pfeifer-Leeg, W. Plass, J. F. Mohr, T. Wichard, H.-P. Saluz and C. Hertweck, Gramibactin is a bacterial siderophore with a diazeniumdiolate ligand system, *Nat. Chem. Biol.*, 2018, DOI: 10.1038/s41589-018-0101-9.
5. S. A. Amin, D. H. Green, M. C. Hart, F. C. Küpper, W. G. Sunda and C. J. Carrano, Photolysis of iron–siderophore chelates promotes bacterial–algal mutualism, *Proc. Natl. Acad. Sci. U. S. A.*, 2009, **106**, 17071-17076.
6. R. Molina, D. Myrold and C. Y. Li, Root symbiosis of red alder : technological opportunities for enhanced regeneration and soil improvement, *The biology and management of red alder*, 1994, 23-46.
7. P. L. Mallet and S. Roy, The symbiosis between *Frankia alni* and alder shrubs results in a tolerance of the environmental stress associated with tailings from the Canadian oil sands industry, *J. Pet. Environ. Biotechnol.*, 2014, **5**.
8. M. M. Georgiadis, H. Komiya, P. Chakrabarti, D. Woo, J. J. Kornuc and D. C. Rees, Crystallographic structure of the nitrogenase iron protein from *Azotobacter vinelandii*, *Science*, 1992, **257**, 1653.
9. A. Sen, S. Sur, L. S. Tisa, A. K. Bothra, S. Thakur and U. K. Mondal, Homology modelling of the *Frankia* nitrogenase iron protein, *Symbiosis*, 2010, **50**, 37-44.
10. L. C. Seefeldt, B. M. Hoffman and D. R. Dean, Mechanism of Mo-dependent nitrogenase, *Annual review of biochemistry*, 2009, **78**, 701-722.
11. D. R. Benson and W. B. Silvester, Biology of *Frankia* strains, actinomycete symbionts of actinorhizal plants, *Microbiol. Rev.*, 1993, **57**, 293-319.
12. J. P. Bellenger, T. Wichard, A. B. Kustka and A. M. L. Kraepiel, Uptake of molybdenum and vanadium by a nitrogen-fixing soil bacterium using siderophores, *Nat. Geosci.*, 2008, **1**, 243-246.
13. J. P. Bellenger, T. Wichard, Y. Xu and A. M. L. Kraepiel, Essential metals for nitrogen fixation in a free-living N2-fixing bacterium: chelation, homeostasis and high use efficiency, *Environ. Microbiol.*, 2011, **13**, 1395-1411.
14. T. Wichard, B. Mishra, S. C. B. Myneni, J.-P. Bellenger and A. M. L. Kraepiel, Storage and bioavailability of molybdenum in soils increased by organic matter complexation, *Nat. Geosci.*, 2009, **2**, 625.
15. C. Jouogo Noumsi, N. Pourhassan, R. Darnajoux, M. Deicke, T. Wichard, V. Burrus and J.-P. Bellenger, Effect of organic matter on nitrogenase metal cofactors homeostasis in Azotobacter vinelandii under diazotrophic conditions, *Environ. Microbiol. Rep.*, 2015, **8**, 76-84.
16. T. Wichard, J.-P. Bellenger, A. Loison and A. M. L. Kraepiel, Catechol siderophores control tungsten uptake and toxicity in the nitrogen-fixing bacterium *Azotobacter vinelandii*, *Environ. Sci. Technol.*, 2008, **42**, 2408-2413.
17. A. M. L. Kraepiel, J. P. Bellenger, T. Wichard and F. M. M. Morel, Multiple roles of siderophores in free-living nitrogen-fixing bacteria, *BioMetals*, 2009, **22**, 573.
18. S. M. Kraemer, O. W. Duckworth, J. M. Harrington and W. D. C. Schenkeveld, Metallophores and trace metal biogeochemistry, *Aquatic Geochemistry*, 2015, **21**, 159-195.
19. R. M. Boiteau, S. J. Fansler, Y. Farris, J. B. Shaw, D. W. Koppenaal, L. Pasa-Tolic and J. K. Jansson, Siderophore profiling of co-habitating soil bacteria by ultra-high resolution mass spectrometry, *Metallomics*, 2018, DOI: 10.1039/C8MT00252E.
20. R. C. Hider and X. Kong, Chemistry and biology of siderophores, *Nat. Prod. Rep.*, 2010, **27**, 637-657.

21. T. R. Furnholm and L. S. Tisa, The ins and outs of metal homeostasis by the root nodule actinobacterium *Frankia*, *BMC Genomics*, 2014, **15**, 1092.

22. M. Rehan, T. Furnholm, R. H. Finethy, F. Chu, G. El-Fadly and L. S. Tisa, Copper tolerance in *Frankia* sp. strain EuI1c involves surface binding and copper transport, *Appl. Microbiol. Biotechnol.*, 2014, **98**, 8005-8015.

23. M. Arahou, H. G. Diem and A. Sasson, Influence of iron depletion on growth and production of catechol siderophores by different *Frankia* strains, *World J. Microbiol. Biotechnol.*, 1997, **14**, 31-36.

24. A. Singh, A. K. Mishra, S. S. Singh, H. K. Sarma and E. Shukla, Influence of iron and chelator on siderophore production in *Frankia* strains nodulating *Hippophae salicifolia* D. Don, *J. Basic Microbiol.*, 2008, **48**, 104-111.

25. D. B. Aronson and G. L. Boyer, Frankia produces a hydroxamate siderophore under iron limitation, *J. Plant Nutr.*, 1992, **15**, 2193-2201.

26. G. L. Boyer, S. A. Kane, J. A. Alexander and D. B. Aronson, Siderophore formation in iron-limited cultures of *Frankia* sp strain 52065 and *Frankia* sp strain CeSI5, *Can. J. Bot.-Rev. Can. Bot.*, 1999, **77**, 1316-1320.

27. R. J. Speirs and G. L. Boyer, Analysis of Fe-55 labeled hydroxamate siderophores by high-performance liquid-chromatography, *J. Chromatogr.*, 1992, **537**, 259-267.

28. G. L. Boyer and D. B. Aronson, in *The biochemistry of metal micronutrients in the rhizosphere*, eds. J. Manthey, A. Manthey and D. E. Crowley, Lewis Publishers, Albany, 1994, ch. 4, pp. 41-54.

29. D. W. Udwary, E. A. Gontang, A. C. Jones, C. S. Jones, A. W. Schultz, J. M. Winter, J. Y. Yang, N. Beauchemin, T. L. Capson, B. R. Clark, E. Esquenazi, A. S. Eustaquio, K. Freel, L. Gerwick, W. H. Gerwick, D. Gonzalez, W. T. Liu, K. L. Malloy, K. N. Maloney, M. Nett, J. K. Nunnery, K. Penn, A. Prieto-Davo, T. L. Simmons, S. Weitz, M. C. Wilson, L. S. Tisa, P. C. Dorrestein and B. S. Moore, Significant Natural Product Biosynthetic Potential of Actinorhizal Symbionts of the Genus *Frankia*, as Revealed by Comparative Genomic and Proteomic Analyses, *Appl. Environ. Microbiol.*, 2011, **77**, 3617-3625.

30. S. Roy, D. P. Khasa and C. W. Greer, Combining alders, frankiae, and mycorrhizae for the revegetation and remediation of contaminated ecosystems, *Can. J. Bot.*, 2007, **85**, 237-251.

31. N. Diagne, K. Arumugam, M. Ngom, M. Nambiar-Veetil, C. Franche, K. K. Narayanan and L. Laplaze, Use of *Frankia* and actinorhizal plants for degraded lands reclamation, *Biomed Res. Int.*, 2013, DOI: 10.1155/2013/948258, 9.

32. M. Ngom, R. Oshone, N. Diagne, M. Cissoko, S. Svistoonoff, L. S. Tisa, L. Laplaze, M. O. Sy and A. Champion, Tolerance to environmental stress by the nitrogen-fixing actinobacterium *Frankia* and its role in actinorhizal plants adaptation, *Symbiosis*, 2016, **70**, 17-29.

33. J. L. Hobman and L. C. Crossman, Bacterial antimicrobial metal ion resistance, *J. Med. Microbiol.*, 2015, **64**, 471-497.

34. A. Singh, S. S. Singh, P. C. Pandey and A. K. Mishra, Attenuation of metal toxicity by frankial siderophores, *Toxicol. Environ. Chem.*, 2010, **92**, 1339-1346.

35. K. J. Waldron and N. J. Robinson, How do bacterial cells ensure that metalloproteins get the correct metal?, *Nature Review: Microbiology*, 2009, **7**, 25-35.

36. I. N. Zelko, T. J. Mariani and R. J. Folz, Superoxide dismutase multigene family: a comparison of the CuZn-SOD (SOD1), Mn-SOD (SOD2), and EC-SOD (SOD3) gene structures, evolution, and expression, *Free Radical Biol. Med.*, 2002, **33**, 337-349.

37. A. Schützendübel and A. Polle, *Plant responses to abiotic stresses: Heavy metal-induced oxidative stress and protection by mycorrhization*, 2002.

38. M. Solioz and J. V. Stoyanov, Copper homeostasis in *Enterococcus hirae*, *FEMS Microbiol. Rev.*, 2003, **27**, 183-195.

39. K. S. E. Abdel-Lateif, S. R. Mansour, M. F. El-Badawy and M. M. Shohayeb, Isolation and molecular characterization of *Frankia* strains resistant to some heavy metals, *J. Basic Microbiol.*, 2018, **58**, 720-729.

23

576 40. M. Deicke, J. F. Mohr, J. P. Bellenger and T. Wichard, Metallophore mapping in complex
577   matrices by metal isotope coded profiling of organic ligands, *Analyst*, 2014, **139**, 6096-6099.
578 41. T. U. H. Baumeister, N. Ueberschaar, W. Schmidt-Heck, J. F. Mohr, M. Deicke, T. Wichard and
579   G. Pohnert, DeltaMS: A tool to track isotopologues in GC- and LC-MS data, *Metabolomics*, 2018,
580   **14:41**.
581 42. T. Wichard and C. Beemelmanns, Role of chemical mediators in aquatic interactions across the
582   prokaryote–eukaryote boundary, *J. Chem. Ecol.*, 2018, **44**, 1008-1021.
583 43. P. A. Belanger, J. Beaudin and S. Roy, High-throughput screening of microbial adaptation to
584   environmental stress, *J. Microbiol. Methods*, 2011, **85**, 92-97.
585 44. M. A. Murry, M. S. Fontaine and J. G. Torrey, Growth kinetics and nitrogenase induction in
586   *Frankia* sp. HFPArI 3 grown in batch culture, *Plant Soil*, 1984, **78**, 61-78.
587 45. B. Schwyn and J. B. Neilands, Universal chemical assay for the detection and determination of
588   siderophores, *Anal. Biochem.*, 1987, **160**, 47-56.
589 46. P. Herzsprung, N. Hertkorn, W. von Tümpling, M. Harir, K. Friese and P. Schmitt-Kopplin,
590   Molecular formula assignment for dissolved organic matter (DOM) using high-field FT-ICR-MS:
591   chemical perspective and validation of sulphur-rich organic components (CHOS) in pit lake
592   samples, *Anal. Bioanal. Chem.*, 2016, **408**, 2461-2469.
593 47. M. Deicke, J. P. Bellenger and T. Wichard, Direct quantification of bacterial molybdenum and
594   iron metallophores with ultra-high-performance liquid chromatography coupled to time-of-flight
595   mass spectrometry, *J. Chromatogr. A*, 2013, **1298**, 50-60.
596 48. E. Butaitė, M. Baumgartner, S. Wyder and R. Kümmerli, Siderophore cheating and cheating
597   resistance shape competition for iron in soil and freshwater *Pseudomonas* communities, *Nat.
598   Comm.*, 2017, **8**, 414.
599 49. F. Zoon, PhD Thesis, Wageningen University, 1995.
600 50. O. Baars, X. Zhang, F. M. M. Morel and M. R. Seyedsayamdost, The siderophore metabolome of
601   *Azotobacter vinelandii*, *Appl. Environ. Microbiol.*, 2016, **82**, 27-39.
602 51. H. Fones and G. M. Preston, The impact of transition metals on bacterial plant disease, *FEMS
603   Microbiol. Rev.*, 2013, **37**, 495-519.
604 52. T. C. Johnstone and E. M. Nolan, Beyond iron: Non-classical biological functions of bacterial
605   siderophores, *Dalton transactions (Cambridge, England: 2003)*, 2015, **44**, 6320-6339.
606 53. A. C. Pozzi, H. H. Bautista-Guerrero, S. S. Abby, A. Herrera-Belaroussi, D. Abrouk, P. Normand,
607   F. Menu and M. P. Fernandez, Robust *Frankia* phylogeny, species delineation and intraspecies
608   diversity based on Multi-Locus Sequence Analysis (MLSA) and Single-Locus Strain Typing
609   (SLST) adapted to a large sample size, *Syst. Appl. Microbiol.*, 2018, **41**, 311-323.
610 54. S. Kodani, M. Ohnishi-Kameyama, M. Yoshida and K. Ochi, A new siderophore isolated from
611   *Streptomyces* sp TM-34 with potent inhibitory activity against angiotensin converting enzyme,
612   *Eur. J. Org. Chem.*, 2011, DOI: 10.1002/ejoc.201100189, 3191-3196.
613 55. C. A. Madigan, T.-Y. Cheng, E. Layre, D. C. Young, M. J. McConnell, C. A. Debono, J. P.
614   Murry, J.-R. Wei, C. E. Barry, G. M. Rodriguez, I. Matsunaga, E. J. Rubin and D. B. Moody,
615   Lipidomic discovery of deoxysiderophores reveals a revised mycobactin biosynthesis pathway in
616   *Mycobacterium tuberculosis*, *Proc. Natl. Acad. Sci. USA*, 2012, **109**, 1257.
617 56. D. C. Young, A. Kasmar, G. Moraski, T.-Y. Cheng, A. J. Walz, J. Hu, Y. Xu, G. W. Endres, A.
618   Uzieblo, D. Zajonc, C. E. Costello, M. J. Miller and D. B. Moody, Synthesis of
619   dideoxymycobactin antigens presented by CD1a reveals T cell fine specificity for natural
620   lipopeptide structures, *J. Biol. Chem.*, 2009, **284**, 25087-25096.
621 57. J. J. De Voss, K. Rutter, B. G. Schroeder and C. E. Barry, Iron acquisition and metabolism by
622   mycobacteria, *J. Bacteriol.*, 1999, **181**, 4443-4451.
623 58. E. Hesse, S. O'Brien, N. Tromas, F. Bayer, A. M. Luján, E. M. van Veen, D. J. Hodgson and A.
624   Buckling, Ecological selection of siderophore-producing microbial taxa in response to heavy
625   metal contamination, *Ecol. Lett.*, 2018, **21**, 117-127.

1
2
3
4
5
6
7
8
9
10
11
12
13
14
15
16
17
18
19
20
21
22
23
24
25
26
27
28
29
30
31
32
33
34
35
36
37
38
39
40
41
42
43
44
45
46
47
48
49
50
51
52
53
54
55
56
57
58
59
60

626   59.   G. M. Teitzel, A. Geddie, S. K. De Long, M. J. Kirisits, M. Whiteley and M. R. Parsek, Survival
627   and growth in the presence of elevated copper: transcriptional profiling of copper-stressed
628   *Pseudomonas aeruginosa*, *J Bacteriol*, 2006, **188**, 7242-7256.
629   60.   A. Braud, V. Geoffroy, F. Hoegy, L. A. Mislin Gaëtan and J. Schalk Isabelle, Presence of the
630   siderophores pyoverdine and pyochelin in the extracellular medium reduces toxic metal
631   accumulation in *Pseudomonas aeruginosa* and increases bacterial metal tolerance, *Environ.*
632   *Microbiol. Rep.*, 2010, **2**, 419-425.
633   61.   I. J. Schalk, M. Hannauer and A. Braud, New roles for bacterial siderophores in metal transport
634   and tolerance, *Environ. Microbiol.*, 2011, **13**, 2844-2854.

635

FRIEDRICH-SCHILLER-UNIVERSITÄT JENA

Institut für Anorganische und Analytische Chemie

Dr. Thomas Wichard
Research Group leader

Lessingstr. 8
07743 Jena

Telefon: 0 36 41 9-481 84
Telefax: 0 36 41 9-481 72
E-Mail: Thomas.Wichard@uni-jena.de

Universität Jena · Institute für Anorganische und Analytische Chemie · 07743 Jena, Germany

To the Editor of
Metallomics

Significance to Metallomics

Jena, 29. November 2018

Dear Editor,

We trust that our manuscript fits very well to the scope of *Metallomics* and will meet the interest of the readership.

Metal homeostasis plays a significant role in bacteria-plant interactions in the rhizosphere. Bacteria can acquire trace metals through metallophores for metal-dependent processes like nitrogen fixation and can contribute to alleviating metal stress. To understand how bacterial metallophores contribute to metal management in a rhizosphere, it is necessary to determine the entirety of metal complexing ligands. In this study, we have explored the metallophore production by Frankia (Actinobacteria), a nitrogen-fixing soil bacterium, using metal isotope-coded profiling. Our study has strong implications for the understanding in the role of bacteria for the plant in trace metal acquisition and detoxification.

With best regards

Table of Contents Entry
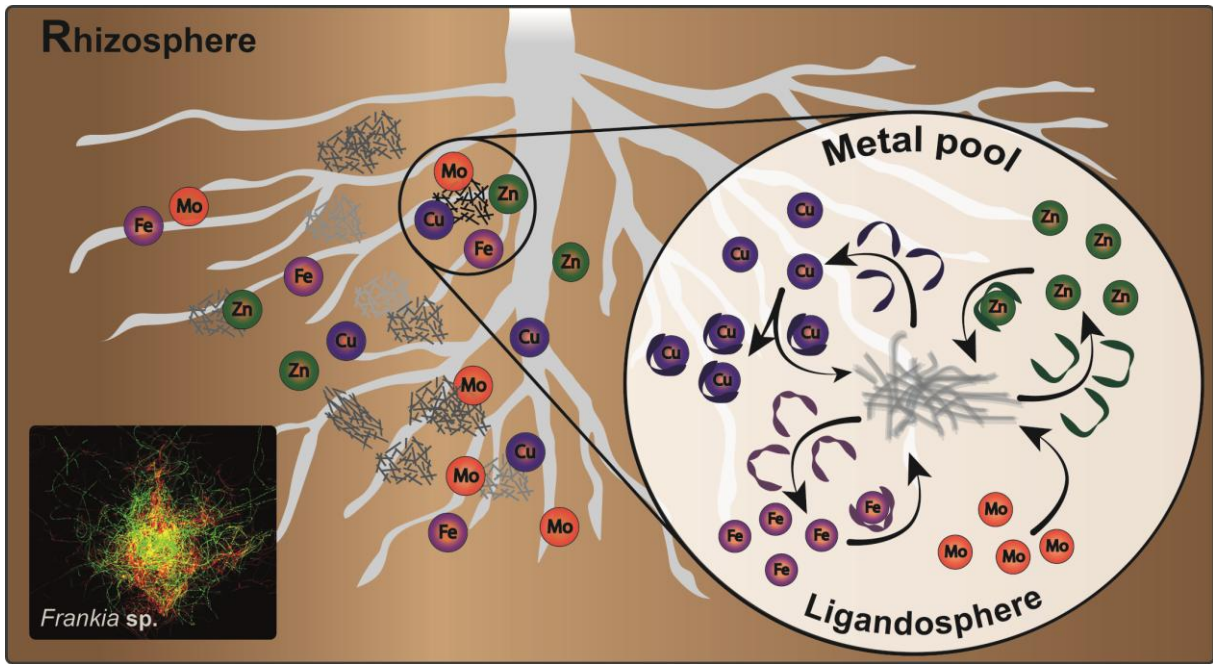
Metal isotope-coded profiling of organic ligands in *Frankia* revealed a high variability of metallophores for trace element acquisition and detoxification.
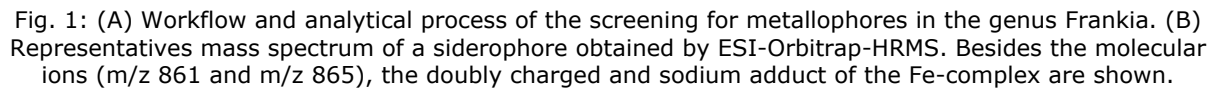
Fig. 1: (A) Workflow and analytical process of the screening for metallophores in the genus Frankia. (B) Representatives mass spectrum of a siderophore obtained by ESI-Orbitrap-HRMS. Besides the molecular ions (m/z 861 and m/z 865), the doubly charged and sodium adduct of the Fe-complex are shown.

207x173mm (300 x 300 DPI)

1
2
3
4
5
6
7
8
9
10
11
12
13
14
15
16
17
18
19
20
21
22
23
24
25
26
27
28
29
30
31
32
33
34
35
36
37
38
39
40
41
42
43
44
45
46
47
48
49
50
51
52
53
54
55
56
57
58
59
60
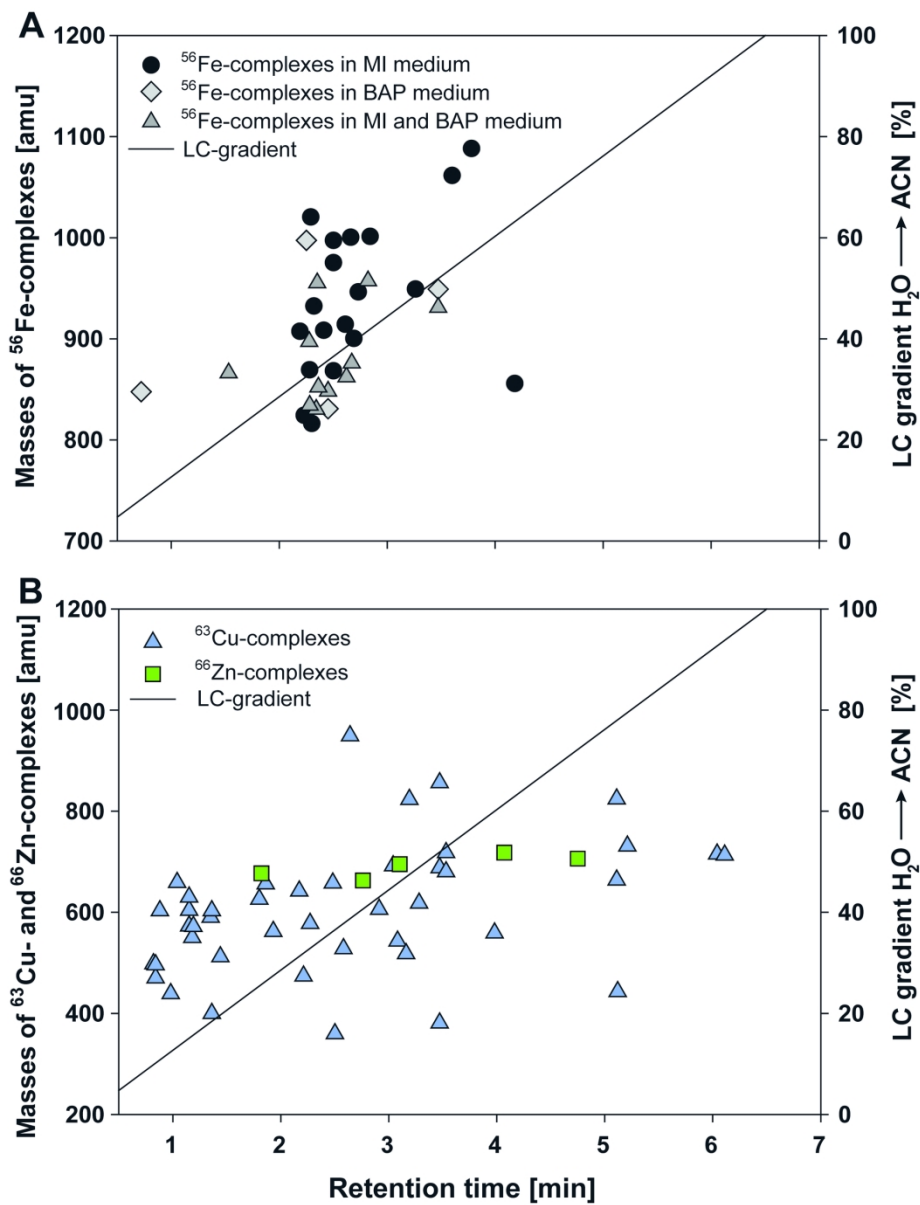
Fig. 2: Plot of m/z values of all detected metallophores over retention time. (A) Fe-complexes determined in Frankia spp. grown in BAP or MI medium. (B) Cu- and Zn complexes determined in Frankia spp. grown in MI medium.

163x213mm (300 x 300 DPI)
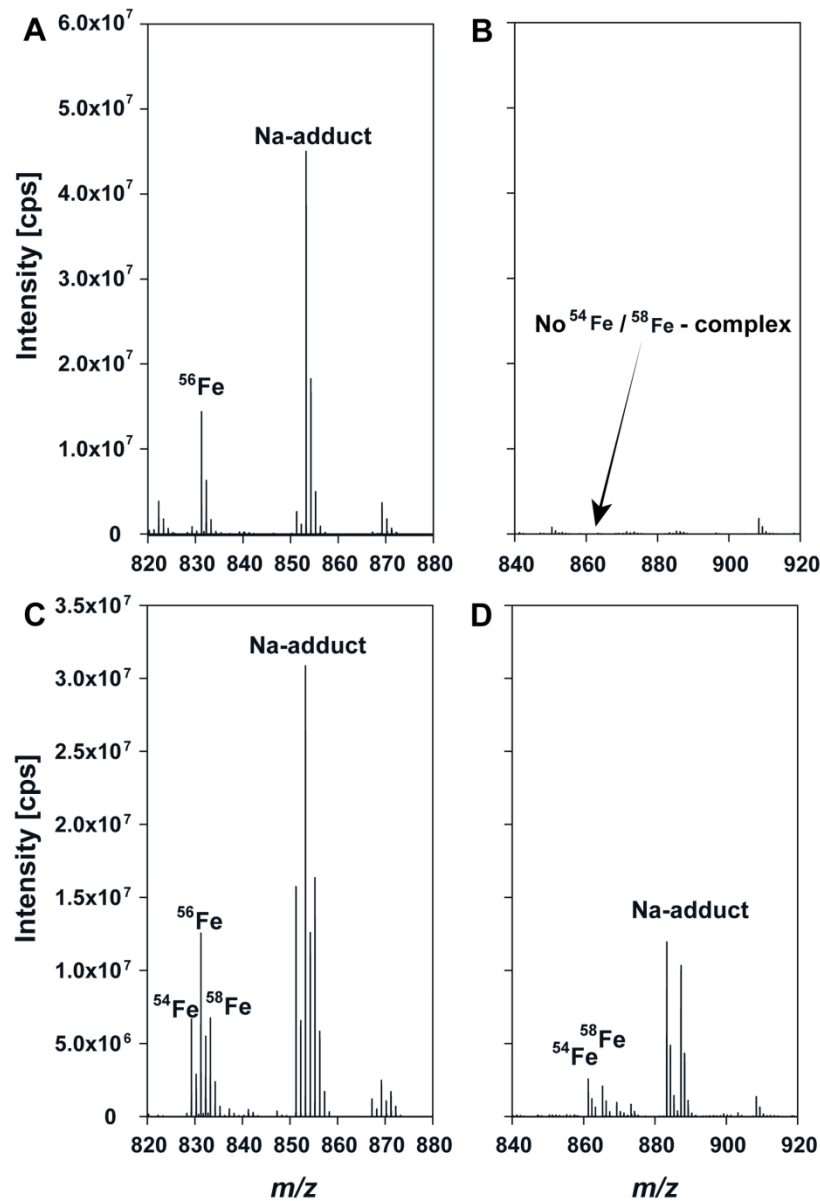
Fig. 3: Characteristic isotopic signature of the ferric complexes for organic ligands of (A, C) type I and (B,D) type II. (A) Type I ligands recruit iron from Fe-EDTA. (B) Type II ligands do not complex iron under standard growth conditions in the presence of Fe-EDTA. Upon addition of 54Fe and 58Fe to the extracts, both (C) type I and (D) type II ligands form iron complexes showing the isotopologues in the ratio 1:1.

144x211mm (300 x 300 DPI)
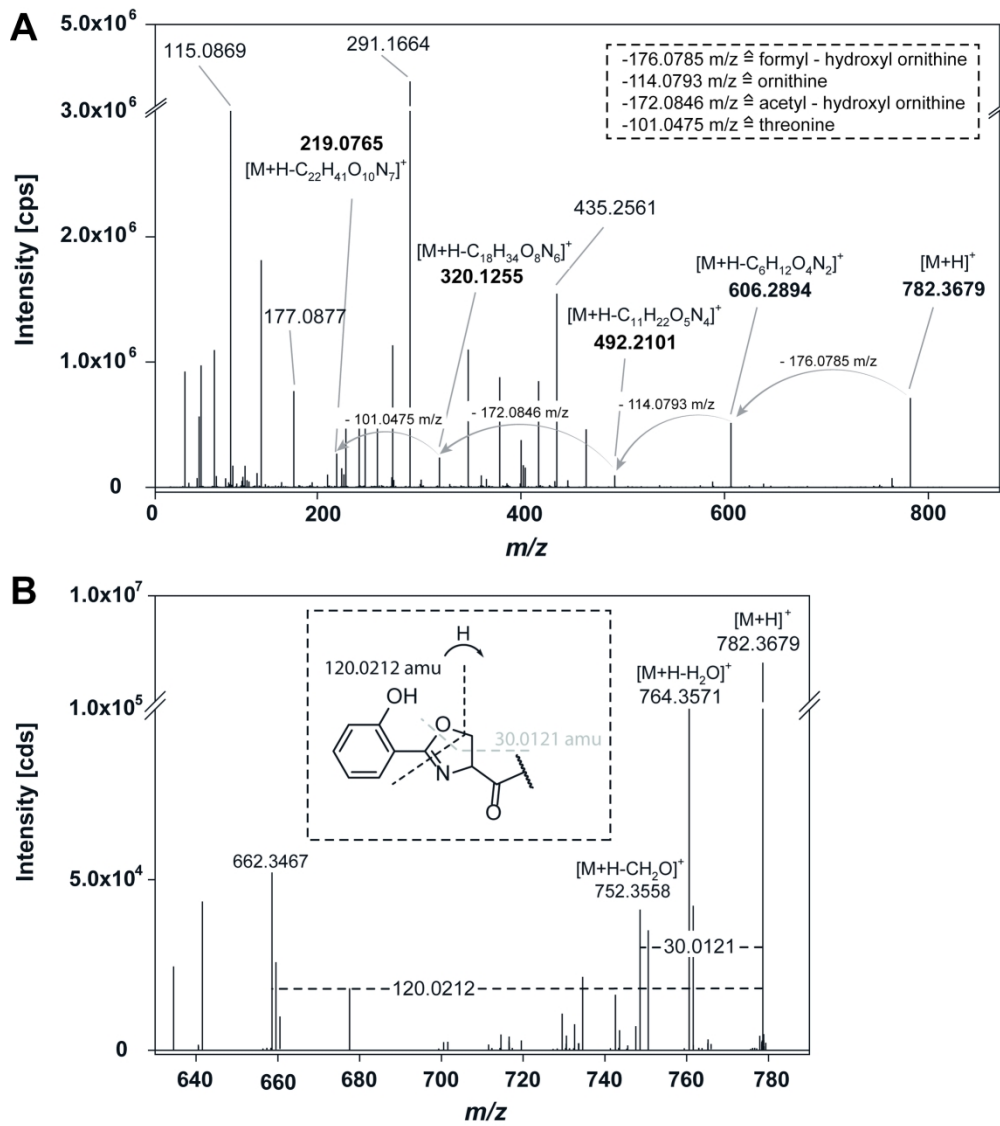
Fig. 4: The electrospray MS/MS mass spectrum (positive mode) for ligand 2 (782 m/z). (A) A typical fragmentation series of the backbone is shown at the collision energy 25 eV. (B) The experiment at the collision energy 20 eV of m/z 782 reveals the characteristic fragmentation of the phenyl-oxazoline-ring.

193x217mm (300 x 300 DPI)
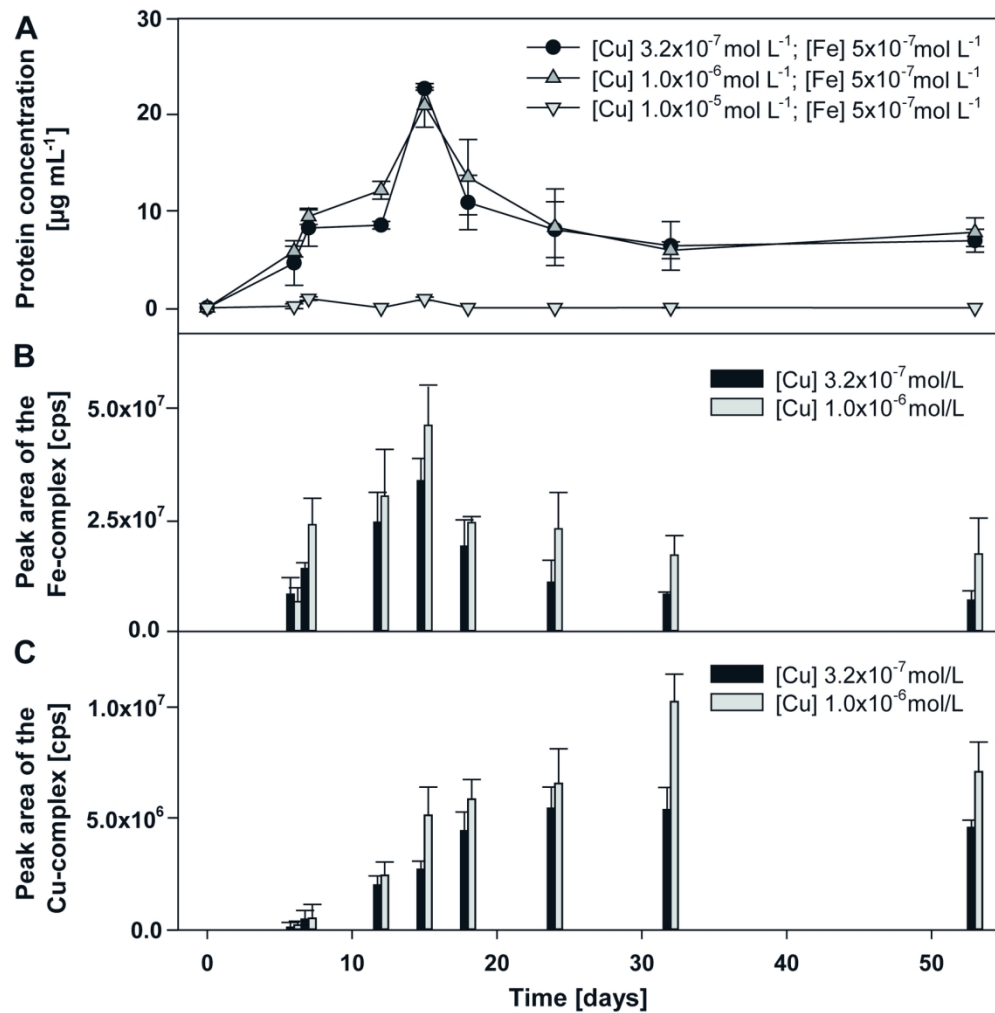
Fig. 5: Time lapse of the growth of Frankia sp. strain CH37 in MI medium. (A) Growth curves are based on total protein content and observed under standard conditions at low, high and toxic Cu concentrations. (B) The relative amounts of the Fe-complex 4 (831 m/z) and (C) Cu-complex 13 (681 m/z) are shown.

153x155mm (300 x 300 DPI)

1
2
3
4
5
6
7
8
9
10
11
12
13
14
15
16
17
18
19
20
21
22
23
24
25
26
27
28
29
30
31
32
33
34
35
36
37
38
39
40
41
42
43
44
45
46
47
48
49
50
51
52
53
54
55
56
57
58
59
60

Supplementary Information for

Metallophore profiling of the nitrogen-fixing genus *Frankia* spp. (Actinobacteria)

towards the understanding of metal acquisition and detoxification in the rhizosphere

Michael Deicke[a‡], Jan Frieder Mohr[a‡], Sébastien Roy[b], Peter Herzsprung[c], Jean-Philippe Bellenger[d], Thomas Wichard[a*]

[a] Friedrich Schiller University Jena, Institute for Inorganic and Analytical Chemistry, Lessingstr. 8, 07743 Jena, Germany.

[b] Centre SÈVE, Département de Biologie, Faculté des Sciences, Université de Sherbrooke, QC, J1K 2R1, Canada

[c] UFZ - Helmholtz Centre for Environmental Research, department Lake Research, Brückstraße 3a, 39114 Magdeburg, Germany

[d] Centre SÈVE, Département de Chimie, Faculté des Sciences, Université de Sherbrooke, QC, J1K 2R1, Canada

‡These authors contributed equally to the manuscript

*corresponding author: Thomas.Wichard@uni-jena.de; Fax: +493641 948172; Tel: +493641 948184

Content

Figure S1: Change of the isotopic signature of metallophores upon addition of Fe, Cu or Zn.
Table S1: Exclusion criteria used for formula assignment.
Table S2: Gradient for the metallophore separation using the UHPLC-HRMS system.
Table S3: Fe-complexes determined in the growth medium of *Frankia* strains.
Table S4: Cu-complexes determined in the growth medium of *Frankia* strains.
Table S5: Zn-complexes determined in the growth medium of *Frankia* strains.

Figures S1: Change of the isotopic signature of the metallophores upon addition of (**A**) ^{56}Fe, (**B**) ^{63}Cu or (**C**) ^{66}Zn. The comparison of the mass spectra shows the decrease in the intensity of free ligand and an increase in the intensity of the respective complex upon addition of the metal. Arrows indicate the change in intensity of the molecular ion peak of the free ligand (down) and a metal complex (up) upon addition of the metal.
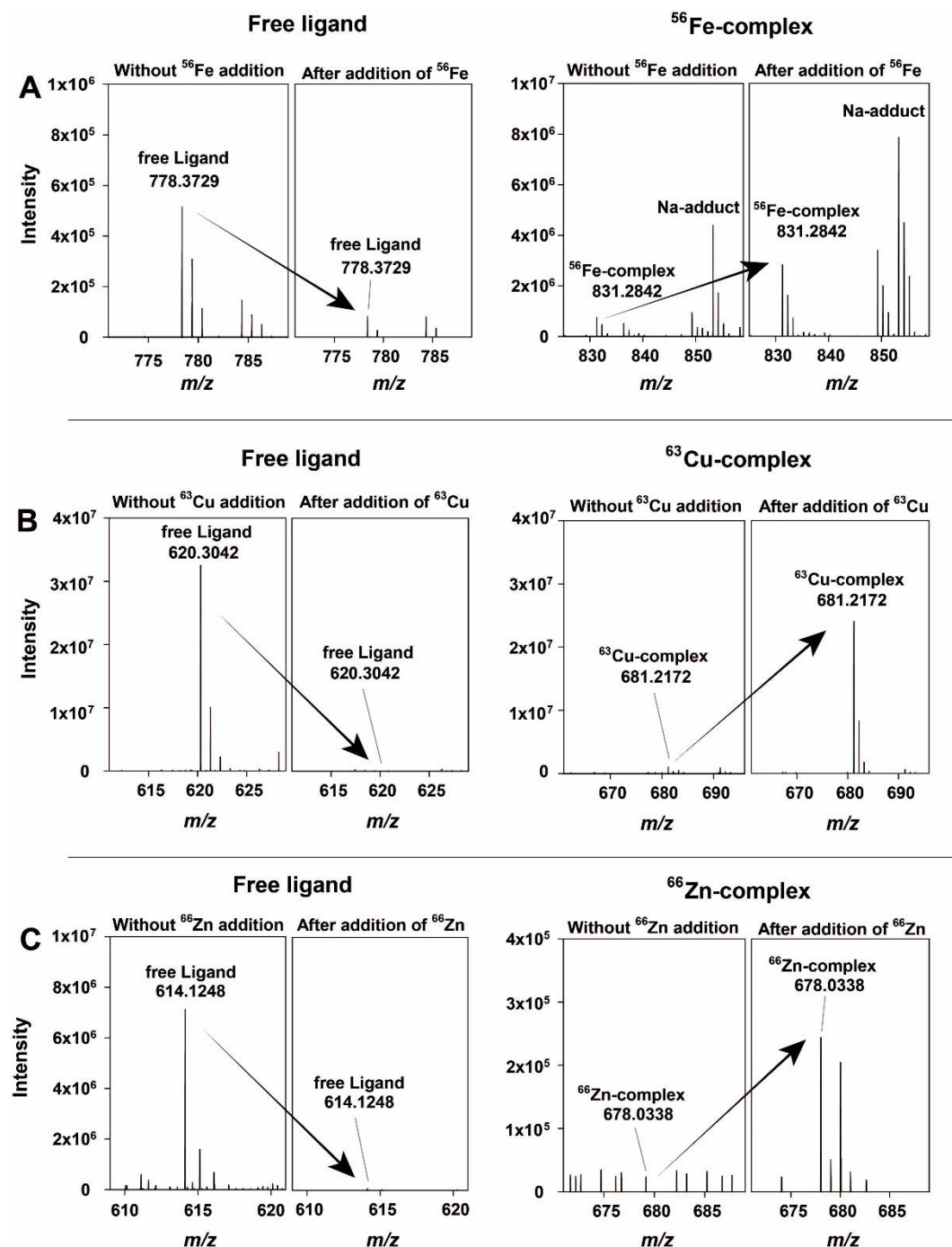
Table S1: Exclusion criteria used for formula assignment; example m/z = 782.3679

[M+H]$^+$ ligand without metal; m/z: 782.3679										
H	**C**	**O**	**N**	**S**	**DBE**	**DBE - O**	**O/N**	**Calc. Mass**	**Δm (ppm)**	**Comment**
52	33	13	9	0	13	0	1.44	782.367912	0.0153	confirmed by fragmentation
62	48	1	0	4	18.5	17.5		782.3678	-0.1278	non-integer DBE
56	41	10	3	1	16	6	3.33	782.368094	0.248	possible
60	26	10	11	3	3	-7	0.91	782.368128	0.2914	low DBE number
62	25	4	14	5	2.5	-1.5	0.29	782.367652	-0.317	non-integer DBE
58	40	4	6	3	15.5	11.5	0.67	782.367618	-0.3604	non-integer DBE
58	33	2	12	4	11.5	9.5	0.17	782.368303	0.5151	non-integer DBE
64	34	7	5	4	6	-1	1.4	782.36831	0.524	too much S
60	33	12	5	2	7	-5	2.4	782.367443	-0.5841	possible
54	32	7	12	2	12.5	5.5	0.58	782.367436	-0.5931	non-integer DBE
56	25	15	11	1	4	-11	1.36	782.367261	-0.8168	DBE – O < -10
52	26	11	15	1	9	-2	0.73	782.368597	0.8909	possible
66	40	3	2	5	9.5	6.5	1.5	782.367149	-0.9599	non-integer DBE
56	34	8	9	2	12	4	0.89	782.368779	1.1235	possible
62	35	13	2	2	6.5	-6.5	6.5	782.368786	1.1325	non-integer DBE
68	33	11	1	4	1	-10	11	782.366974	-1.1836	low DBE number
62	32	6	8	4	6.5	0.5	0.75	782.366967	-1.1925	non-integer DBE
56	31	1	15	4	12	11	0.07	782.36696	-1.2015	DBE – O > +10
58	47	6	0	2	19.5	13.5		782.366933	-1.236	non-integer DBE
58	24	9	14	3	3.5	-5.5	0.64	782.366785	-1.4252	non-integer DBE
54	39	9	6	1	16.5	7.5	1.5	782.366751	-1.4686	non-integer DBE
50	31	12	12	0	13.5	1.5	1	782.366569	-1.7012	non-integer DBE
48	34	9	13	0	18	9	0.69	782.369248	1.723	possible
54	35	14	6	0	12.5	-1.5	2.33	782.369255	1.7319	non-integer DBE
60	46	0	3	4	19	19	0*	782.366457	-1.8444	DBE – O > +10
62	39	8	2	3	10.5	2.5	4	782.366282	-2.0681$^\#$	non-integer DBE
56	38	3	9	3	16	13	0.33	782.366275	-2.077$^\#$	DBE – O > +10
58	31	11	8	2	7.5	-3.5	1.38	782.3661	-2.3007$^\#$	non-integer DBE
52	30	6	15	2	13	7	0.4*	782.366093	-2.3097$^\#$	too low O/N
54	46	11	0	0	20.5	9.5		782.366066	-2.3442$^\#$	non-integer DBE
54	23	14	14	1	4.5	-9.5	1	782.365918	-2.5333$^\#$	non-integer DBE
64	38	2	5	5	10	8	0.4*	782.365806	-2.6765$^\#$	too low O/N

*O/N ratio was too low

Δm, mass error (ppm) = [(m/z (experimental mass) – calc mass)/calc mass] × 1,000,000

$^\#$ |Δm| > 2 ppm

Table S2: Gradient for the metallophore separation using the UHPLC-HRMS system. Eluent A: 1 mmol L^{-1} ammonium acetate in water and 2% (v/v) acetonitrile, eluent B: 1 mmol L^{-1} ammonium acetate in acetonitrile and 10% (v/v) water.

Time [min]	Eluent A [%]	Eluent B [%]
0	100	0
0.20	100	0
8.00	0	100
9.00	0	100
9.10	100	0
10.0	100	0

Table S3: Fe-complexes were determined in the growth medium (MIM or BAP) of various *Frankia* strains using metal isotope-coded profiling. The masses of the uncharged [56]Fe-complex are listed. The positive (+) or negative (-) ionisation mode for determination of the metallophores is stated ([1]: MS-adducts in positive mode; [2]: MS - adducts in the negative mode were also found).

Mass of [56]Fe complex [amu]	Strains	Retention time [min]	MS - polarity mode	Medium
816.2621[1]	CH37	2.3	+/-	MIM
802.2817[1]	CH37, Ea1-12	2.23	+	MIM
830.2758[1,2]	CH37, Cj1-82, BCU 110501, Arl3	2.34	+/-	MIM/BAP
830.8643[1]	Ea1-12	2.45	+	BAP
834.2706[1]	CH37	2.28	+/-	MIM
847.6644	CH37	0.72	-	BAP
848.2881[1,2]	CH37, Ea1-12	2.49	+/-	MIM/BAP
852.2811[1]	CH37	2.36	+/-	MIM/BAP
855.7049	Cj1-82	4.18	-	MIM
862.3039[1]	CH37, Cj1-82, Ea1-12, DC12, BCU 110501	2.62	+/-	MIM/BAP
866.3005	CH37	1.53	-	MIM/BAP
868.2896[1]	BCU 110501	2.5	+	MIM
869.2844	CH37	2.28	+	MIM
876.0527	CcI3 (Lab. Boyer)	2.67	+	MIM/BAP
889.3217	BCU 110510	2.17	+	MIM
897.3525[1]	ACN14a, Cg70.4, Cg70.9, Cj1-82, CcI3 (Lab. Boyer), BCU 110501, Arl3	2.276	+/-	MIM/BAP
900.3190[1]	CH37	2.69	+	MIM
907.3339	BCU 110501	2.19	-	MIM
908.3227	CH37	2.41	+	MIM
914.3357[1,2]	CH37	2.61	+/-	MIM
931.1315[1]	BCU 110501	3.47	+	MIM/ BAP
932.3462[1]	CH37	2.32	+/-	MIM
946.3645[1]	CH37	2.73	+	MIM
949.1409[1]	BCU 110501	3.47	+	BAP
949.1431[1]	CcI3 (Lab. Boyer)	3.26	+	MIM
955.3100	CcI3 (Lab. Boyer)	2.35	+	MIM/BAP
957.3159[1,2]	CH37, ACN14a, Ea1-12, CcI3 (Lab. Boyer), CcI3 (Univ. Laval)	2.82	+/-	MIM/BAP
975.3268	ACN14a	2.5	-	MIM
997.3093	ACN14a	2.5	-	MIM
997.3495[1]	Arl3	2.25	+	BAP
1000.3334	CH37	2.66	-	MIM
1001.2795	ACN14a	2.84	+	MIM
1020.3536	CH37	2.29	-	MIM
1061.4418	CH37	3.6	+	MIM
1088.2085	BCU 110501	3.78	+	MIM

Table S4: Cu-complexes were determined in the growth medium (MIM) of various *Frankia* strains using metal isotope-coded profiling. The positive (+) or negative (-) ionisation mode for determination of the metallophores is stated.

Mass of ^{63}Cu^{II}- complex [amu]	Strains	Retention time [min]	MS - polarity mode
359.9941	CH37	2.5	+
381.0737	CH37	3.47	+
400.0545	CH37, ACN14a	1.36	+
439.0904	CH37	0.98	+
443.0677	CH37	5.12	+
470.1214	CH37	0.84	+
474.0236	ACN14a	2.21	+/-
496.1117	CH37	0.84	+
498.1278	CcI3 (Univ. Laval)	0.82	+
512.1459	CcI3 (Lab. Boyer)	1.44	+
518.0977	CH37	3.16	+
528.1746	CH37	2.58	+
543.0931	CH37	3.08	+
550.0962	ACN10a, ACN12a, ACN14a, CcI3 (Lab. Boyer), CH37, Cg70.4	1.18	+
559.1607	CH37	3.98	+/-
562.1913	CcI3 (Univ. Laval), CcI3 (Lab. Boyer)	1.93	+/-
572.0781	DSMZ 44251	1.19	+
573.1224	CH37	1.15	+
578.0930	ACN14a	2.27	+/-
590.0657	CJ1-82, CcI3 (Lab. Boyer)	1.35	+
603.1154	CH37	1.36	+
603.1710	CcI3 (Lab. Boyer)	0.88	+
604.1539	CH37	1.15	+/-
606.1226	CH37	2.91	+
618.1736	CH37, DC12	3.28	+/-
626.1258	Cg70.9, CcI3 (Univ. Laval)	1.8	+
630.1442	CH37	1.15	+
642.0742	CH37	2.17	+/-
656.1363	Ea1-12	1.86	+
658.0673	CH37	2.48	+
659.0783	CcI3 (Univ. Laval)	1.04	+
663.9572	CH37	5.11	+/-
680.20891	CH37	3.53	+
688.1754	CH37	3.47	+/-
692.1723	ACN14a	3.04	+/-
713.1699	Cg70.4	6.11	+
715.1819	CcI3 (Univ. Laval), CH37, BCU 110501	6.04	+
718.1645	CH37	3.53	+
731.1791	CPI1	5.21	+/-
823.2669	CH37	3.19	+
824.2145	CH37	5.11	+/-
856.2882	CH37	3.47	+
949.3090	ACN14a	2.64	+/-

1
2
3
4
5
6
7
8
9
10
11
12
13
14
15
16
17
18
19
20
21
22
23
24
25
26
27
28
29
30
31
32
33
34
35
36
37
38
39
40
41
42
43
44
45
46
47
48
49
50
51
52
53
54
55
56
57
58
59
60

Table S5: Zn-complexes were determined in the growth medium (MIM) of various *Frankia* strains using metal isotope-coded profiling. The positive (+) or negative (-) ionisation mode for determination of the metallophores is stated.

Mass of $^{66}Zn^{2+}$- complex [amu]	Strains	Retention time [min]	MS - Polarity
663.146	CcI3 (Lab. Boyer)	2.76	+
677.0263	BCU 110501	1.82	+
695.1709	ACN14a	3.1	+/-
706.3383	ACN12a	4.75	+
718.1749	ACN12a, CcI3 (Lab. Boyer), CH37	4.07	+/-

1
2
3
4
5
6
7
8
9
10
11
12
13
14
15
16
17
18
19
20
21
22
23
24
25
26
27
28
29
30
31
32
33
34
35
36
37
38
39
40
41
42
43
44
45
46
47
48
49
50
51
52
53
54
55
56
57
58
59
60